

Tin oxide films grown over glass and KBr at several substrate temperatures

D. R. ACOSTA

U.N.A.M, Instituto de Física, Apdo. Postal. 20-364, 01000 Mexico D.F., Mexico

A. MALDONADO, R. ASOMOZA

CINVESTAV Departamento de Ingeniería Eléctrica, Apdo. Postal 14-740, 07000 Mexico D.F., Mexico

Tin oxide films were deposited by spray pyrolysis on KBr and glass substrates. Conventional and high-resolution electron microscopy were used to determine grain sizes, atomic arrays and crystallographic details present in the films as a function of the growing parameters used. Optical and electrical properties were also measured and related to the structural details observed. The existence of SnO and Sn₃O₄ phases was revealed in films obtained at low substrate temperatures.

1. Introduction

The properties of high transparency and high conductivity found in SnO₂ thin films have promoted a wide investigation oriented to technological developments. Their use has been extended to heaters, anti-static films and anti-reflecting coatings in solar cells, among others [1]. Moreover, SnO₂ is also an excellent active material for semiconductor gas sensors. However, a comprehensive understanding of the detailed nature of the composition and the structure, which affect the optical properties and transport mechanism of these films, is still lacking. The optical and electrical properties of SnO₂ films are dependent on their microstructure, including structural defects, orientation of the grains and morphology. Crystalline orientation and morphology are, in turn, affected by the deposition mechanism and parameters involved in the process.

A number of deposition techniques are employed to obtain SnO₂ thin films, which have been reviewed recently [2]. The properties of the films depend on the conditions of preparation and vary considerably from one technique to another. Chemical spray pyrolysis is a simple and low-cost technique to obtain good-quality films, in a reproducible way and at relatively low temperatures. It is therefore a good option for preparing SnO₂ films when they are an integral part of a device.

In this work chemical spray pyrolysis was used to prepare SnO₂ thin films on glass and KBr. The dependence of the structure and morphology of these films on the deposition parameters was investigated by using high-resolution electron microscopy (HREM) and conventional electron microscopy (CTEM) at 400 and 100 kV, respectively. These techniques allowed us to obtain structural details at the unit cell level. The optical and electrical properties, studied by standard methods, are also reported. We

correlated, when possible, the observed characteristics with the deposition conditions in order to obtain the best films regarding uniformity, transparency and conductivity. In polycrystalline films an increase in grain size is important to obtain lower values of the resistivity by decreasing the free carrier scattering at the grain boundaries [3]. The phases present, morphologies and particle size distributions were also studied in our samples.

2. Experimental procedure

SnO₂ thin films were obtained by spraying a 0.2 M solution of stannic chloride, dissolved in ethyl alcohol, on to KBr and glass substrates, in an open air atmosphere. The substrate temperatures used were 300, 400 and 450 °C. In order to obtain uniform substrate temperatures a molten tin bath 3 in. (76 mm) in diameter was used. Nitrogen was used as carrier gas at a fixed rate of 4 l min⁻¹; the solution rate was adjusted to 3.2 ml min⁻¹. The substrate temperature was continuously measured with a Chromel-Alumel thermocouple in contact with the surface of the molten tin bath; temperature variations during growing were kept within ± 5 °C. The thickness was determined both optically and by the colour of the film, during the growth, due to light interference within the sample. Typical thicknesses were of the order of 230 nm. A more detailed explanation on the growth system can be found elsewhere [4].

Films grown on KBr were used for electron microscopy studies and resistivity measurements. Films grown on glass were used to measure the electrical resistivity and optical transmittance.

Those grown on KBr crystallites were released by flotation in distilled water and mounted directly on 200 mesh copper grids without a carbon supporting film. After drying they were mounted in an analytical

side-entry Jeol 100 CX microscope, equipped with a goniometer and operated at 100 kV, as well as in an ultra-high resolution Jeol 4000 EX electron microscope equipped with a $C_s = 1.0$ mm pole-piece and operated at 400 kV. Electrical characterization was carried out by the four-probe method in films deposited on both kinds of substrate. Optical properties were determined from the transmission pattern, taken with a Perkin Elmer Lambda 4 spectrophotometer, in the 350–750 nm range, which is the characteristic operation region of a solar cell. The analysis of the data was based on the method reported by Manificier *et al.* [5].

3. Results and discussion

Fig. 1 shows the resistivity, as a function of substrate temperature, for films deposited on both substrates, KBr and glass. In both cases the resistivity reaches a minimum around 400 °C. The resistivity of the films grown on KBr was higher due, certainly, to a high content of alkaline ions coming from the substrate, which compensate the free charge carriers.

Transmittance patterns for films obtained on glass substrates are shown in Fig. 2. As can be seen, the transmittance increases as the substrate temperature increases, possibly as a consequence of a more efficient formation of stoichiometric SnO₂. This will be discussed later.

Figs 3 and 4 show transmission electron microscopy images obtained from the sample prepared at $T_s = 300$ °C (sample 1). Fig. 3 is a bright-field CTEM image in which a high density of very uniform size grains, around 18 nm, can be appreciated. This image suggests a uniform growing process as the sprayed

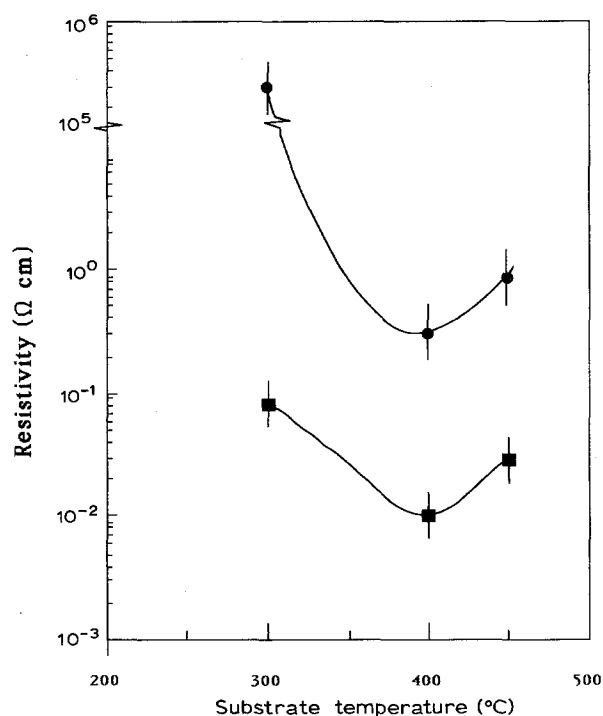


Figure 1 Resistivity versus substrate temperature for SnO₂ films deposited on (●) KBr crystallites and (■) glass.

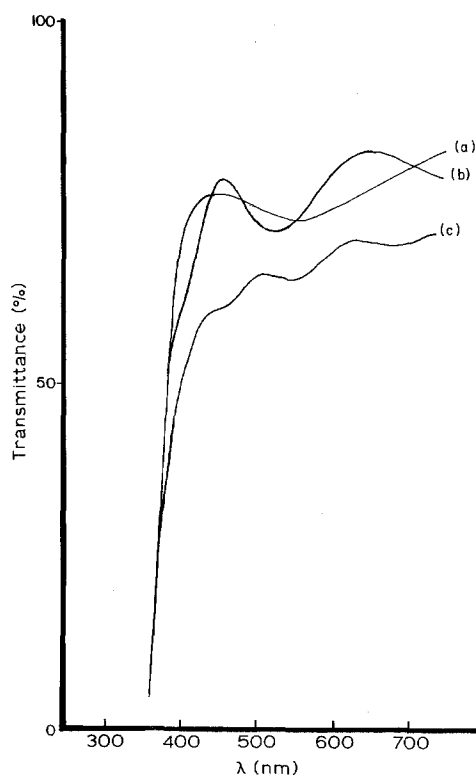


Figure 2 Transmittance patterns for films grown on glass substrates at different temperatures: (a) $T_s = 450$ °C (b) $T_s = 400$ °C and (c) $T_s = 300$ °C.

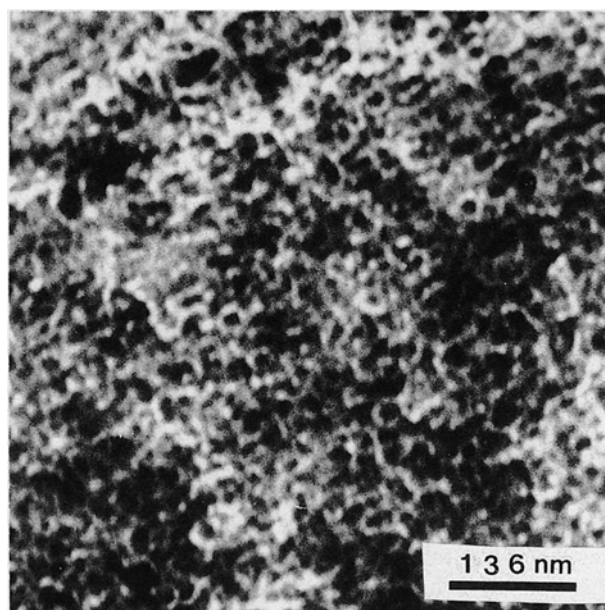


Figure 3 Low-magnification CTEM image from sample 1 ($T_s = 300$ °C). High grain density and uniformity can be appreciated.

solution reaches the substrate. Fig. 4 shows a high-resolution image from which a relatively high degree of crystallinity can be deduced; however, the zones indicated by the arrows show the presence of non-crystalline regions corresponding, probably, to the initial growing layers, which according to Fujimoto *et al.* [6] can be associated with an amorphous precursor phase.

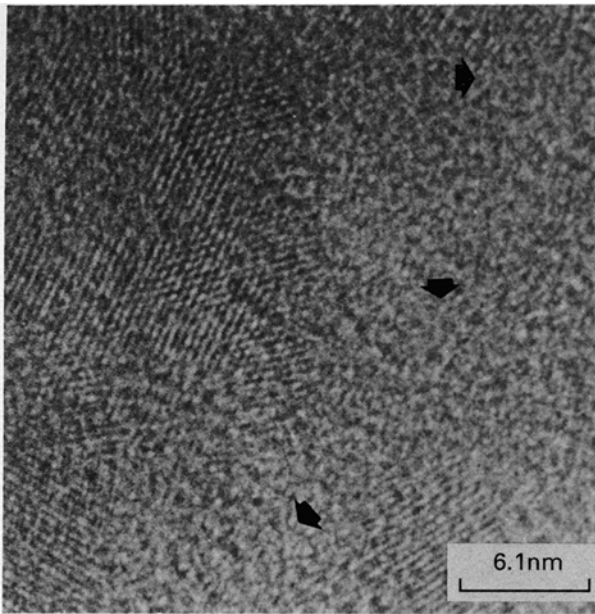


Figure 4 HREM image from sample 1 where, besides crystalline regions of SnO₂, some amorphous zones can be observed.

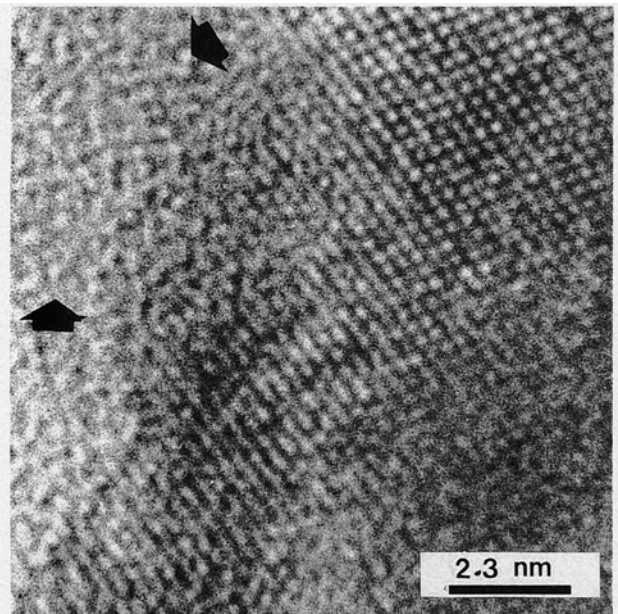


Figure 6 HREM image from sample 2 where crystalline and amorphous zones can be clearly distinguished.

Figs 5 and 6 are images obtained from the sample prepared at 400 °C (sample 2). Three relevant details can be distinguished in Fig. 5:

1. A low-contrast support (marked A) which might correspond to the first layers of amorphous SnO₂ mentioned before.
2. Dark rounded details (marked B) which corresponds to SnO₂ grains with different sizes which begin to agglomerate to form the film.
3. Rounded clear details (marked C) which might correspond to places in the low-contrast support where the particles marked B were temporarily stationed before reaching their final location.

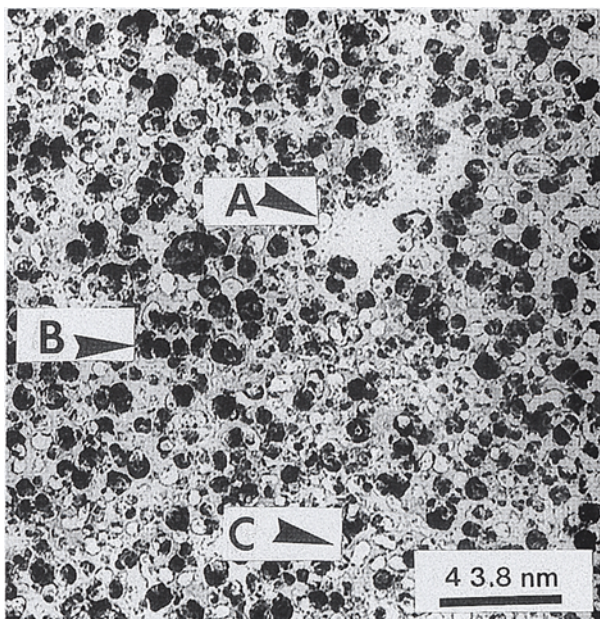


Figure 5 CTEM image of sample 2 ($T_s = 400\text{ }^\circ\text{C}$) where several different features (explained in the text) can be observed.

Fig. 6 shows an HREM image coming from a region close to an edge of sample 2. A high degree of crystallinity was observed; however, an amorphous zone indicated by the arrows was again detected.

Figs 7 and 8 correspond to bright- and dark-field images obtained from the same zone of the sample prepared at 450 °C (sample 3). It can be observed that the crystal grows over a non-diffracting background corresponding to low-contrast zones, which again could be associated with an amorphous precursor layer. Fig. 8 was obtained using the (0 2 0) reflection of a ring selected-area electron diffraction pattern (SAED). This image indicates that the SnO₂ film is formed by grains in different crystallographic orientations.

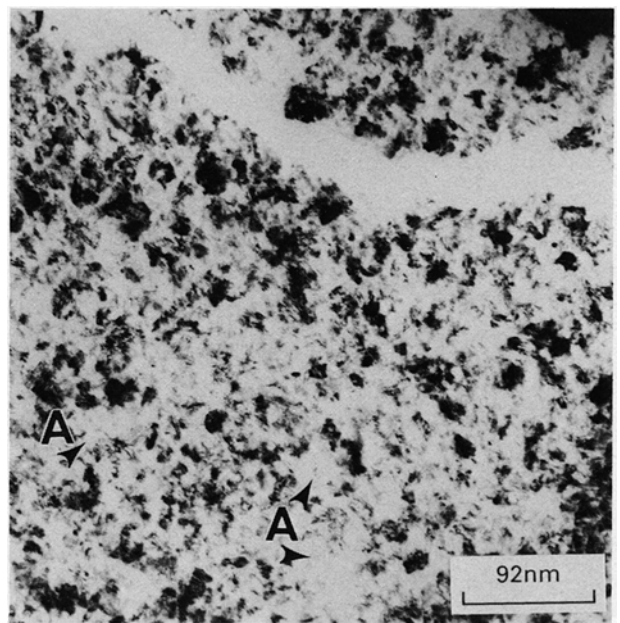


Figure 7 CTEM bright-field image from sample 3 ($T_s = 450\text{ }^\circ\text{C}$) showing several big grains over an apparent amorphous zone (marked with arrow).

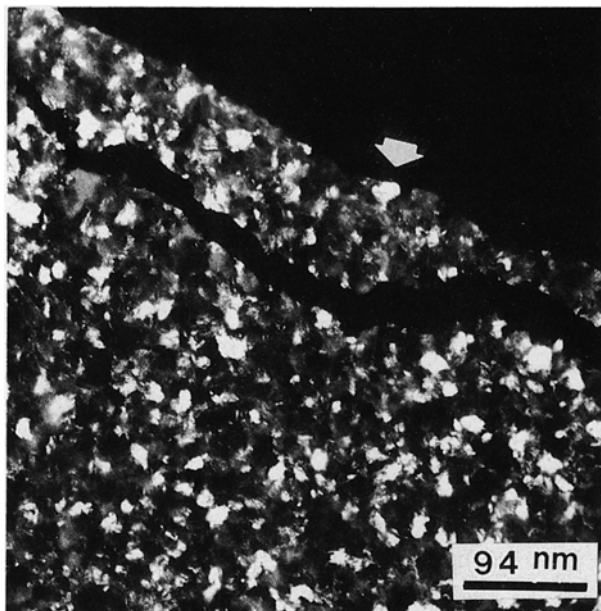


Figure 8 CTEM dark-field image of the zone presented in Fig. 7; individual small grains and clustered grains can be observed.

Fig. 9 is an HREM image from sample 3 where, besides a high degree of crystallinity, several structural features such as dislocations, twinings, grain boundaries and different grain orientations can be observed. This image suggests that droplets from the sprayed solution undergo many dynamic interactions during the deposition process, before reaching the substrate and also at the substrate, depending on the flow rate.

Figs 10, 11 and 12 correspond to SAED patterns coming from samples 1, 2, and 3, respectively. The crystalline structure and cell parameters were deduced from these pictures and others not shown. Patterns from samples 1 and 2 fit perfectly with tetragonal SnO_2 , with cell parameters $a = 0.472 \text{ nm}$ and $c = 0.313 \text{ nm}$. The same values were obtained from ring

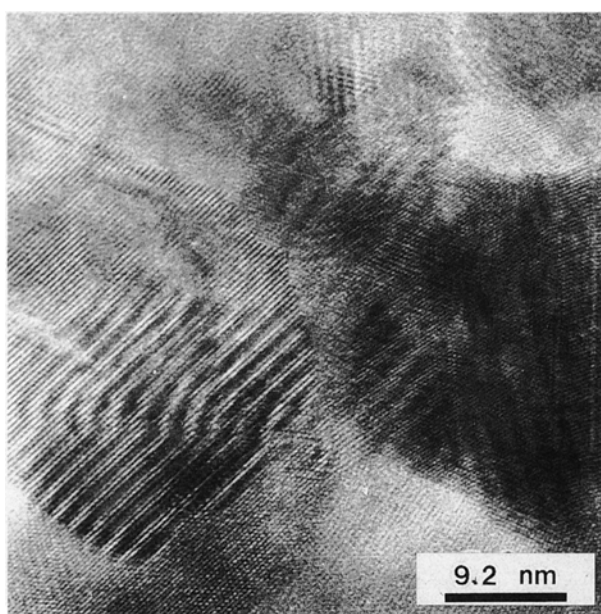


Figure 9 HREM image from sample 3 where the polycrystalline nature of the SnO_2 film is readily recognized: grains, grain boundaries and other structural defects can also be observed.

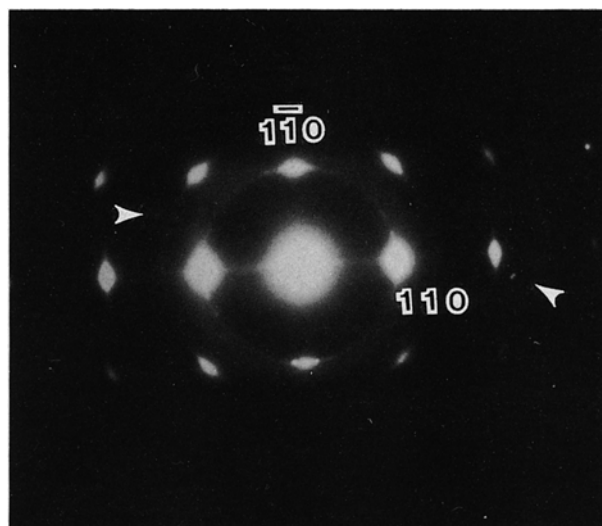


Figure 10 Selected-area electron diffraction patterns from sample 1 corresponding to SnO_2 . The elongation of some spots suggests some kind of shape effects in the SnO_2 film.

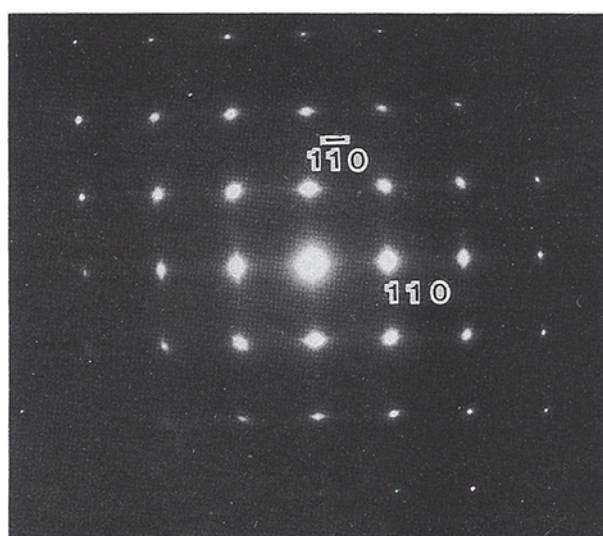


Figure 11 SAED pattern from sample 2 where a high degree of crystallinity for SnO_2 obtained at 400°C is appreciated.

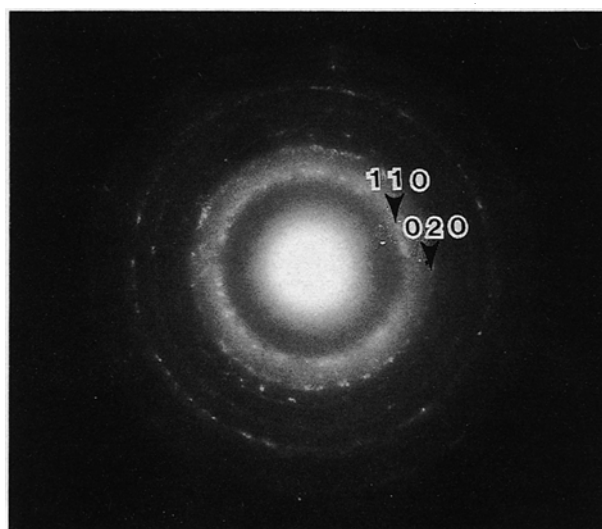


Figure 12 SAED pattern from polycrystalline sample 3. This kind of pattern was found everywhere in this sample.

TABLE I Grain size distributions

Sample	T_s (°C)	Size distribution (nm)
1	300	$6.0 < d < 36.5$
2	400	$6.5 < d < 87.5$
3	450	$15.0 < d < 110.0$

patterns (Fig. 12) coming from sample 3. The presence of extra ordered spots in Figs 10 and 11 led us to conclude the existence of other stannic oxides in samples 1 and 2. These phases were identified as SnO and Sn₃O₄.

Grain size distributions of films grown on KBr are reported in Table I. The crystallite sizes were obtained from CTEM and HREM images. It can be observed that the average grain size increases as the substrate temperature increases.

From measurements carried out on HREM images between many pairs of SnO₂ grains, it was found that there is not a systematic preferred orientation for the three samples studied in this work; this implies the absence of epitaxial phenomena during the growing processes.

TEM results show the presence of a non-diffracting layer in all samples, even in those prepared at 450 °C. Embedded in this amorphous material, TEM images revealed the presence of high-quality crystalline regions which at 300 °C correspond to small SnO₂ crystals (see Table I), mixed with SnO and Sn₃O₄. These crystalline regions grow as the substrate temperature increases. At the highest T_s used, 450 °C, the only compound remaining is nearly stoichiometric polycrystalline SnO₂, as evidenced by TEM results (Fig. 12). It is estimated that at low substrate temperature the small particles arriving at the substrate nucleate easily and grow smoothly, giving rise to highly ordered regions connected by an amorphous tissue. In addition, at low temperature the chemical reaction producing SnO₂ is not complete, giving as a result SnO and Sn₃O₄, as evidenced by the diffraction patterns. At the highest temperature used, the more efficient evaporation of the solvent as well as the higher energy of the species at the substrate surface produce a more complete reaction which decreases the amount of phases other than SnO₂, but gives rise to crystallites with a high density of structural defects.

The effect of grain boundary scattering on the electrical resistivity has been studied by Seto [7] in polycrystalline silicon. According to his model, the resistivity is expected to decrease as the grain size increases. This behaviour is observed in our samples at low substrate temperatures; however, we observed a minimum in the resistivity at about 400 °C because the composition in films prepared at 450 °C approaches the stoichiometric composition of SnO₂, which is a

highly transparent insulator. This result also explains the high transparency of these films on disappearance of the other phases, SnO and Sn₃O₄, present when low substrate temperatures were used.

4. Conclusions

Nearly stoichiometric SnO₂ thin films having the cassiterite structure have been obtained at high substrate temperature. At low substrate temperature the presence of other stannic oxides was also detected.

From CTEM and HREM images it was found that an amorphous material coexists with the crystalline phases, even at the highest substrate temperatures. This amorphous layer may be related to a precursor phase in the growth of SnO₂ films. The differences in grain size distribution as a function of substrate temperature can be attributed to variations in the thermodynamic parameters during the nucleation and growth processes. Samples prepared at 450 °C show a great number of structural defects (grain boundaries, twins, dislocations, etc.) not observed in the other samples.

Selected-area diffraction patterns show that samples 1 and 2 contain single-crystalline regions, while sample 3 is polycrystalline. From SAED and HREM there was no evidence of epitaxial growth on to the KBr crystalline support.

The resistivity of the films is consistent with grain boundary scattering and the optical transmittance reveal a higher transparency for films obtained at higher substrate temperature, which can be related to a more efficient formation of stoichiometric tin oxide at high temperature.

Acknowledgements

The technical assistance of Mr Luis Rendón and Mr Alfredo Sánchez in electron microscopy and photographic work, respectively, is recognized.

References

1. J. B. MOONEY and S. B. RADDING, *Ann. Rev. Mater. Sci.* **12** (1982) 81.
2. S. OKTIK, *Prog. Cryst. Growth Charac.* **17** (1988) 171.
3. N. S. MURTY and S. R. JAWALEKAR, *Thin Solid Films* **102** (1983) 283.
4. A. TIBURCIO SILVER, MSc thesis, Electrical Engineering Department, CIEA, IPN, Mexico (1985).
5. J. C. MANIFACIER, J. GASLOT and J. P. FILLARD, *J. Phys. E: Sci. Instrum.* **9** (1976) 1002.
6. M. FUJIMOTO, T. URANO, S. MURAI and Y. NISHI, *Jap. J. Appl. Phys.* **28** (1989) 2587.
7. J. Y. W. SETO, *J. Appl. Phys.* **46** (1966) 247.

Received 29 April

and accepted after revision 11 September 1992